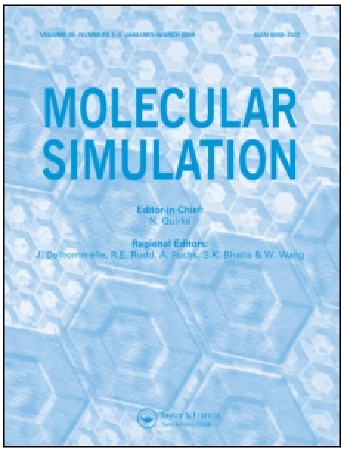

Molecular Simulation
Publication details, including instructions for authors and subscription information:
http://www.informaworld.com/smpp/title~content=t713644482

The Rheology of 6-Propyl Duodecane and 5-Dibutyl Nonane by Non-Equilibrium Molecular Dynamics Simulations

Song Hi Lee[a]
[a] Department of Chemistry, Kyungsung University, Pusan, Korea

To cite this Article Lee, Song Hi(1999) 'The Rheology of 6-Propyl Duodecane and 5-Dibutyl Nonane by Non-Equilibrium Molecular Dynamics Simulations', Molecular Simulation, 22: 4, 271 — 284

To link to this Article: DOI: 10.1080/08927029908022101

URL: http://dx.doi.org/10.1080/08927029908022101

Molecular Simulation, 1999, Vol. 22, pp. 271 – 284
Reprints available directly from the publisher
Photocopying permitted by license only

Published by license under
the Gordon and Breach Science
Publishers imprint.
Printed in Malaysia.

THE RHEOLOGY OF 6-PROPYL DUODECANE AND 5-DIBUTYL NONANE BY NON-EQUILIBRIUM MOLECULAR DYNAMICS SIMULATIONS

SONG HI LEE

Department of Chemistry, Kyungsung University, Pusan, Korea 608-736

(Received January 1999; accepted February 1999)

In recent papers, we reported non-equilibrium molecular dynamics (NEMD) simulations of planar Couette flow for liquid *n*- and *i*-butane, and liquid *n*-decane and 4-propyl heptane, using two collapsed atom models and an atomistically detailed model. It was found that the collapsed atom models predict the viscosities of the *n*-butane and *n*-decane quite well, and that the atomistically detailed model does not yield quantitative agreement with the viscosity of the *n*-alkanes or the branched alkanes, but it does have the one positive feature that the calculated viscosities of the branched alkanes are higher than those of the *n*-alkanes. In the present paper, we report results of NEMD simulations of planar Couette flow for liquid 6-propyl duodecane and 5-dibutyl nonane at 296 K and 0.782 g/cc, using an expanded collapsed atom model for simplicity. The strain rate dependent viscosity shows three different regions – two shear thinning ones and a Newtonian one. The slopes of the log-log plot for the branched-chain alkanes at high strain rate are different from those at intermediate strain rate, which is characterized as a rheological behavior of branched-chain alkanes. The Newtonian viscosity of the branched-chain alkanes can be extrapolated from the plateau value of the strain rate dependent viscosity at low strain rate as for straight-chain alkanes [*J. Chem. Phys.*, **105**, 1214 (1996)]. The results indicate that more-branched alkanes have a larger viscosity than less-branched C_{17} alkanes.

Keywords: Viscosity; non-equilibrium molecular dynamics simulation; 6-propyl duodecane; 5-dibutyl nonane; expanded collapsed atom model

I. INTRODUCTION

There is growing interest in understanding the rheological properties of linear alkanes of moderate size (C_4-C_{20}) by using non-equilibrium molecular dynamics (NEMD) [1 – 5] simulations of Couette flow. In general calculated viscosities from NEMD simulations are in reasonably good agreement with experimental values. However, only recently has the viscosity of branched alkanes been studied by NEMD simulations. NEMD simulations of Lennard-Jones (LJ) site-site models representing *n*-butane and *i*-butane were performed over much of the density range for which experimental data are available, by Rowley and Ely [6]. Simulated viscosities at zero shear agreed very well with experimental data over the entire density range. Site-size, non-equilibrium molecular alignment and molecular geometry were the primary factors causing both the similarities and differences between isomers' viscosity and rheology.

Evans and his coworkers have used NEMD simulations to study the rheological behavior of linear and branched alkanes, *n*-tridecane and 5-butyl nonane [4], using the Weeks-Chandler-Andersen (WCA) prescription [7, 8] for the site-site LJ potential. The general features of the results were in agreement with recent simulations of *n*-decane and *n*-eicosane [3], but the details of the results differed for linear and branched alkanes. For example, the general trend of decreasing viscosity at low shear rates followed by an increase in the viscosity at higher strain rates was once again observed, but the viscosity for the linear alkane was always less than that of the branched alkane.

Cummings and his coworkers have carried out extensive NEMD simulations for liquid *n*-decane, *n*-hexadecane, and *n*-tetracosane at densities corresponding to atmospheric pressure and near ambient temperatures [9]. They found that at high strain rate, the viscosities for all the three *n*-alkanes have similar values and exhibits similar power-law shear-thinning behavior with a slope between about −0.40 and −0.33 and that at low strain rate, the shear viscosity shows a transition to Newtonian behavior and the Newtonian viscosity can be obtained from the plateau value of the shear viscosity at the lowest strain rates calculated from the NEMD simulations.

Lee and Cummings have reported NEMD simulations of planar Couette flow of liquid C_4 alkanes (*n*-butane and *i*-butane) [10] and C_{10} alkanes (*n*-decane and 4-propyl heptane) [11] using two collapsed atom models and an atomistically detailed model [12 – 14]. They found that the collapsed atomic models predict the viscosities of *n*-butane and *n*-decane quite well in general agreement with previous workers [2, 6, 15 – 17] but if these models are applied to the isomers, the viscosity is underpredicted. They also found that their atomistically detailed model does not yield quantitative agreement with the viscosity of the *n*-butane or the *i*-butane or the *n*-decane or the 4-propyl heptane. However this model has the one positive feature that the calculated viscosities of branched alkanes (*i*-butane and 4-propyl heptane) are higher than those of *n*-alkanes (*n*-butane and *n*-decane) as observed experimentally (branching increases the viscosity). The results suggest that the inclusion of *H* atoms may be important in correctly predicting the effect of molecular structure on physical properties of liquid alkanes.

In this paper, we examine the Newtonian and strain rate dependent rheological properties of two branched C_{17} alkanes, 6-propyl duodecane and 5-dibutyl nonane, using the expanded collapsed atom model [15, 18]. The original Ryckaert-Bellemans collapsed atom model [19, 20] is not used since the results of the two collapsed models are very similar [10, 11] and also the atomistically detailed model [12–14] is not used since the C_{17} alkane systems are too large to simulate with various strain rates. The main goal here is to investigate the branching effect on the rheological properties of the C_{17} alkanes. The number of branches differed for the two C_{17} alkanes. Does the subtle difference of the two C_{17} alkanes in the degree of branching affect their rheological properties?

The paper is organized as follows. Section II contains a brief description of molecular models and MD simulation methods followed by Section III which presents the results of our simulations and Section IV where our conclusions are summarized.

II. MOLECULAR MODEL AND MOLECULAR DYNAMICS SIMULATIONS

The molecular model adopted for 6-propyl duodecane and 5-dibutyl nonane is here called the expanded collapsed atomic model. Monomeric units are treated as single spheres with masses of 14.145 g/mole. They interact through an LJ potential between the spheres in different molecules and between the spheres more than three apart on the same molecule. The C—C—C—C torsional rotational potential is given by the original Ryckaert-Bellemans form [19]:

$$V(\phi) = c_0 + c_1 \cos\phi + c_2 \cos^2\phi + c_3 \cos^3\phi + c_4 \cos^4\phi + c_5 \cos^5\phi \qquad (1)$$

where Φ is the C—C—C—C dihedral angle. The LJ parameters and c_i's are listed in Table I.

This model also includes the C—C bond stretching and C—C—C bond angle bending potentials in addition to the LJ and torsional potentials of the above Ryckaert-Bellemans potential:

$$V_b(r_{ij}) = K_0(r_{ij} - r_e)^2 \qquad (2)$$

TABLE I Potential parameters for the expanded collapsed atom model of liquid alkanes

LJ parameters	σ(nm)	ε(kJ/mol)				
site–site	0.3923	0.5986				
torsional	co(kJ/mol)	c_1	c_2	c_3	c_4	c_5
C—C—C—C	9.279	12.136	−13.120	−3.060	26.240	−31.495
bond stretching	r_e(nm)		K_0(kJ/mol nm^2)			
C—C	0.153		132600			
bond angle bending	θ_e(deg)		K_1(kJ/mol deg^2)		K_2(kJ/mol deg^3)	
C—C—C	109.47		0.05021		0.000482	

$$V_a(\theta) = K_1(\theta - \theta_e)^2 - K_2(\theta - \theta_e)^3 \tag{3}$$

The equilibrium bond length (r_ε) and bond angle (θ_e), and the force constants (K_0, K_1 and K_2) are used by Chynoweth *et al.* [15, 18] which are originally provided by the work of White and Boville [21], and are given in Table I.

For the study of planar Couette flow, in which fluids are subjected to homogeneous shear between two parallel plates, the NEMD algorithm for alkane is a molecular version of the SLLOD algorithm [22], The equations of motion for site s in molecule i are given by

$$\frac{d\boldsymbol{r}_{\text{is}}}{dt} = \frac{\boldsymbol{p}_{\text{is}}}{m_s} + \boldsymbol{n}_x \gamma y_i \tag{4}$$

$$\frac{d\boldsymbol{p}_{\text{is}}}{dt} = \boldsymbol{F}_{\text{is}} - \boldsymbol{n}_x \frac{m_s}{M} \gamma p_{yi} - \alpha \frac{m_s}{M} \boldsymbol{p}_i \tag{5}$$

where $M = \sum_s M_s$, $\boldsymbol{r}_i = \sum_s (m_s/M)\boldsymbol{r}_{\text{is}}$, and $\boldsymbol{F}_i = \sum_s \boldsymbol{F}_{\text{is}}$. $\boldsymbol{n}_x$ is the unit vector in the x-direction, $\boldsymbol{F}_{\text{is}}$ is the force exerted by the other sites in the same and different molecules on the site s in molecule i, γ is the strain rate, $\partial u_x/\partial y$, and α is the thermostatting constant, given by

$$\alpha = \frac{\sum_{i=1}^{N} [\boldsymbol{F}_i \cdot \boldsymbol{p}_i - \gamma p_{yi} p_{xi}]}{\sum_{i=1}^{N} p_i^2} \tag{6}$$

The effect of the thermostatting term involving $\gamma(m_s/M)\boldsymbol{p}_i$ in Eq. (5) is to hold the translational center-of-mass kinetic energy constant. The momenta is Eqs. (4) and (5) are measured with respect to the streaming velocity of the fluid and are known as peculiar momenta.

The pressure tensor $\boldsymbol{P}$ is expressed in terms of molecular quantities by

$$\boldsymbol{P}V = \sum_{i=1}^{N} \frac{\boldsymbol{p}_i \boldsymbol{p}_i}{M} + \sum_{1 \le i \le j < N} \sum \boldsymbol{r}_{ij} \boldsymbol{F}_{ij} \tag{7}$$

where V is the volume of the system, $\boldsymbol{r}_{ij} = \boldsymbol{r}_i - \boldsymbol{r}_j$ is the vector joining the centers of molecules i and j, and $\boldsymbol{F}_{ij}$ is the force between them. These equations of motion are combined with the Lees-Edwards "sliding brick" boundary conditions [23]. In the absence of the thermostat, the terms in Eqs. (4) and (5) involving the strain field, γ, cancel to yield Newton's equations of motion relating $\boldsymbol{r}_i$ and $\boldsymbol{F}_i$. This implies that the SLLOD algorithm truly generates boundary driven planar Couette flow, leading to the conclusion that it is correct to arbitrary order in the strain rate when appropriately thermostatted [24]. The strain rate dependent shear viscosity is then obtained from Newton's law of viscosity

$$\eta = -\frac{P_{xy} + P_{yx}}{2\gamma} \tag{8}$$

where P_{xy} and P_{yx} are the averaged xy and yx components of $\boldsymbol{P}$.

A canonical ensemble of fixed $N(= 27$ molecules), V(length of cubic box, $L = 2.398\,\mathrm{nm}$), and $T(T = 296\,\mathrm{K})$ is chosen for the simulation ensemble. Gauss's principle of least constraint [25, 26] is used to maintain the system at a constant temperature according to Eqs. (5) and (6). A spherical cut-off of radius $R_c = 2.5\,\sigma$, where σ is the LJ parameter, was employed for all the pair interactions. For the integration over time, we adopted Gear's fifth-order predictor–corrector algorithm [27] with a time step of 0.0005 ps. A total of 1,000,000 time steps was simulated each for the average and the configurations of molecules were stored every 10 times steps for further analysis.

III. RESULTS AND DISCUSSION

In Figure 1, the strain rate dependent viscosities of the expanded collapsed atom model of 6-propyl duodecane and 5-dibutyl nonane at 296 K and 0.782 g/cc are plotted. Detailed numerical data and production run lengths are tabulated in Table II with the calculated pressures. We have plotted the figure on a log–log scale and the strain rate covers several orders of magnitude. The viscosity shows three different regions – two shear thinning

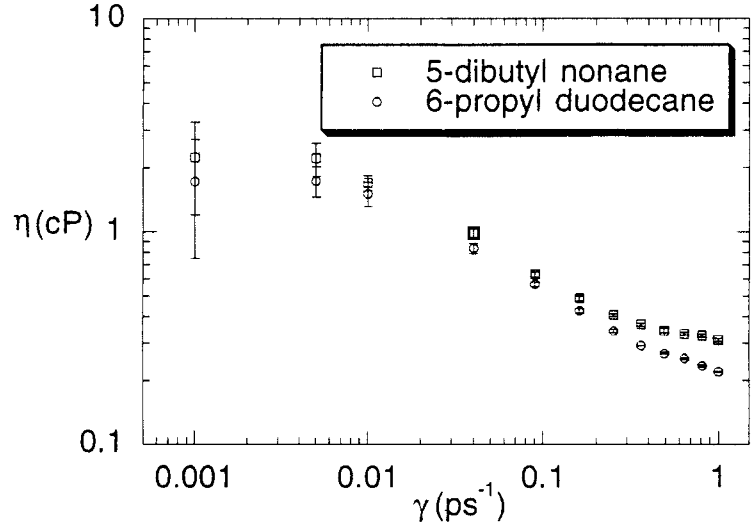

FIGURE 1 The strain rate dependent viscosity (cP) for 6-propyl duodecane and 5-dibutyl nonane at 296 K and 0.782 g/cc.

TABLE II The viscosity and pressure for the expanded collapsed atom model of 6-propyl duodecane and 5-dibutyl nonane at various strain rates obtained from our NEMD simulations at 296 K and 0.782 g/cc

Run length(ns)	$\gamma(ps^{-1})$	*6-propyl duodecane* $\eta(cP)$	*6-propyl duodecane* $P(bar)$	*5-dibutyl nonane* $\eta(cP)$	*5-dibutyl nonane* $P(bar)$
4.4	0.001	1.732 ± 0.984	−344.5 ± 25.5	2.236 ± 0.535	−290.8 ± 33.0
4.4	0.005	1.742 ± 0.285	−319.2 ± 31.6	2.233 ± 0.392	−254.2 ± 33.2
2.8	0.01	1.514 ± 0.204	−275.8 ± 29.2	1.705 ± 0.143	−196.0 ± 18.9
2.8	0.04	0.839 ± 0.046	−139.2 ± 12.5	0.990 ± 0.051	33.7 ± 40.4
2.0	0.09	0.570 ± 0.013	−10.6 ± 14.2	0.631 ± 0.016	184.1 ± 44.8
2.0	0.16	0.426 ± 0.011	112.3 ± 19.9	0.487 ± 0.013	357.6 ± 34.2
1.6	0.25	0.341 ± 0.006	204.2 ± 28.8	0.406 ± 0.006	538.5 ± 6.2
1.6	0.36	0.292 ± 0.002	380.4 ± 6.8	0.367 ± 0.007	849.3 ± 39.0
1.6	0.49	0.269 ± 0.003	731.7 ± 19.1	0.344 ± 0.009	1299.0 ± 68.4
1.2	0.64	0.254 ± 0.002	1198.0 ± 44.4	0.332 ± 0.005	1943.3 ± 50.5
1.2	0.81	0.234 ± 0.003	1668.1 ± 25.2	0.325 ± 0.005	2776.8 ± 60.1
1.2	1.00	0.220 ± 0.002	2299.8 ± 13.9	0.311 ± 0.005	3617.1 ± 99.7

ones and a Newtonian one. At high strain rate (0.36 ~ 1.0 ps^{-1}), the slopes of the log-log plot are −0.277 and −0.162 for 6-propyl duodecane and 5-dibutyl nonane, respectively, and at intermediate strain rate (0.01 ~ 0.25 ps^{-1}), the slopes are −0.463 and −0.446, respectively. For polymer fluids, the experimentally observed slopes are −0.4 to −0.9 of shear shinning typically. This suggests that the branched-chain alkanes studied here show somewhat different behavior from the generality of the long-chain systems.

More significant difference is appeared in the behavior at high strain rate, where the strain rate dependent viscosities for 6-propyl duodecane and 5-dibutyl nonane are of substantial difference. This is exactly opposite to the observation in the NEMD simulation study of straight-chain alkanes (*n*-decane, *n*-hexadecane, and *n*-tetracosane) [9], in which the shear viscosities for the straight-chain alkanes at high strain rate nearly overlap each other and this behavior is related to the fact that at high strain rate, these fairly short and stiff alkane chains are well aligned with each other so they can slide past each other easily. Here, however, the situation is very different: in the branched-chain alkanes, there are multiply imposed torsional rotational potentials. For example, 3 doubly and 4 triply imposed dihedral states exist on each central site of 6-propyl duodecane and 5-dibutyl nonane, respectively. When the main backbone chains of the branched-chain alkanes align with each other along the shear at high strain rate, the branched chains prevent them from sliding past each other easily and the prevention degree differs in 6-propyl duodecane and 5-dibutyl nonane due to the multiplicity of the imposed dihedral states as seen in the slopes of the log – log plot at high strain rate from Figure 1. This is the main difference between the straight-chain and the branched-chain alkanes.

At low strain rate ($0.001 \sim 0.005\,\mathrm{ps}^{-1}$), the increase of viscosity with decreasing strain rate stops and the data points indicates some plateau behavior, suggesting the appearance of a Newtonian region of the viscosity. This is exactly the same behavior observed in the NEMD simulation study of straight-chain alkanes [9]. Based on the shear viscosity at the lowest strain rate, the extrapolated Newtonian viscosity is estimated to be 1.73 ± 0.98 and 2.24 ± 0.54 cP for 6-propyl duodecane and 5-dibutyl nonane at 296 K and 0.782 g/cc, respectively. More-branched alkanes have a larger viscosity than less-branched C_{17} alkanes. These values are consistent with those for *n*-hexadecane obtained from the NEMD simulation study of straight-chain alkanes [9]: 1.63 ± 0.28 cP at 300 K and 0.770 g/cc, and 1.24 ± 0.12 cP at 323 K and 0.753 g/cc. The viscosities calculated by integrating the stress auto-correlation functions *via* the Green-Kubo relations using equilibrium molecular dynamics (EMD) simulation are underestimated (0.612 and 0.787 cP for 6-propyl duodecane and 5-dibutyl at 296 K and 0.782 g/cc, respectively) [14], but it shows the same trend that branching increases viscosity.

There are various methods for the extrapolation to zero strain rate to obtain the Newtonian viscosity [28]. From kinetic and mode coupling theories [29 – 31], it is known that for simple atomic fluids [32 – 34] and small chain molecules [1 – 6, 10, 11, 15], the strain rate dependence of the shear viscosity is linear in $\gamma^{1/2}$. Hence, to apply the SLLOD algorithm to a Newtonian fluid, one performs several simulations at different strain rates γ and fits the resulting strain rate dependent viscosities to the equation

$$\eta = \eta_0 + \eta_1 \gamma^{1/2}, \tag{9}$$

where the zero strain rate extrapolation of η, η_0, is thus the Newtonian viscosity. For liquid alkanes, the power law behavior of the viscosity *vs* strain rate indicate a qualitatively difference between the dynamical behaviors of the long-chain alkanes and small chain molecules, and a further difference between those of the straight-chain and the branched-chain alkanes which are observed in this study. The experimental evidence for polymer liquids suggests that the viscosity *vs* strain rate is Newtonian at low strain rate and follows a power law shear shinning at high strain rate. Therefore, it is more desirable to use the plateau value of the viscosity at very low strain rate for the Newtonian viscosity.

Figure 2 shows the strain rate dependent pressure difference of 6-propyl duodecane and 5-dibutyl nonane at 296 K and 0.782 g/cc. Detailed numerical data and production run lengths are tabulated in Table II. The equilibrium pressure at zero strain rate is negative for both 6-propyl duodecane

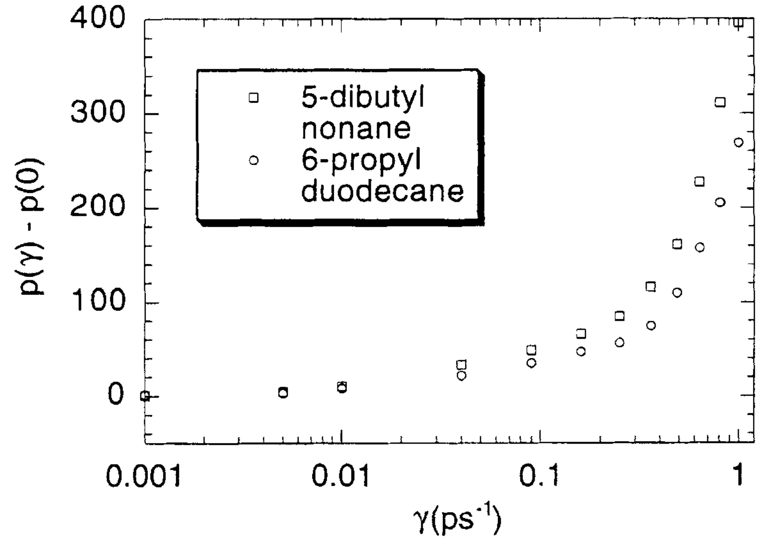

FIGURE 2 The strain rate dependent pressure difference (atm) for 6-propyl duodecane and 5-dibutyl nonane at 296 K and 0.782 g/cc (1 atm = 1.01325 bar = 0.101325 MPa).

and 5-dibutyl nonane. At low strain rate, the pressure is nearly equal to the equilibrium pressure and at relatively high strain rate, the pressure increases nearly linearly with the strain rate. For simple atomic liquids, both mode coupling theory and simulations suggest that the pressure, p, and the configuration energy, E_{conf}, satisfy the asymptotic relations

$$p = p_0 + p_1\gamma^{3/2} \text{ and } E_{\mathrm{conf}} = E_0 + E_1\gamma^{3/2}. \qquad (10)$$

At high strain rate ($0.36 \sim 1.0\,\mathrm{ps}^{-1}$), when the pressure of both 6-propyl duodecane and 5-dibutyl nonane is plotted *vs* $\gamma^{3/2}$ (not shown), it shows a 3/2 power law, but at low strain rate ($< 0.25\,\mathrm{ps}^{-1}$), the pressure *vs* $\gamma^{3/2}$ does not follow a straight line. Because of the complexity of the chain molecules, there is no reason to expect the theory for simple atomic systems to be applicable to these systems. Recent computer simulations have produced a variety of behavior for shear dilatancy of hydrocarbon chain liquids [3, 35]. For our MD simulations of 6-propyl duodecane and 5-dibutyl nonane, the shear dilatancy does not show significant dependence on strain rate.

The strain rate dependent normal stress difference is plotted in Figure 3 for 6-propyl duodecane and 5-dibutyl nonane at 296 K and 0.782 g/cc. Bird

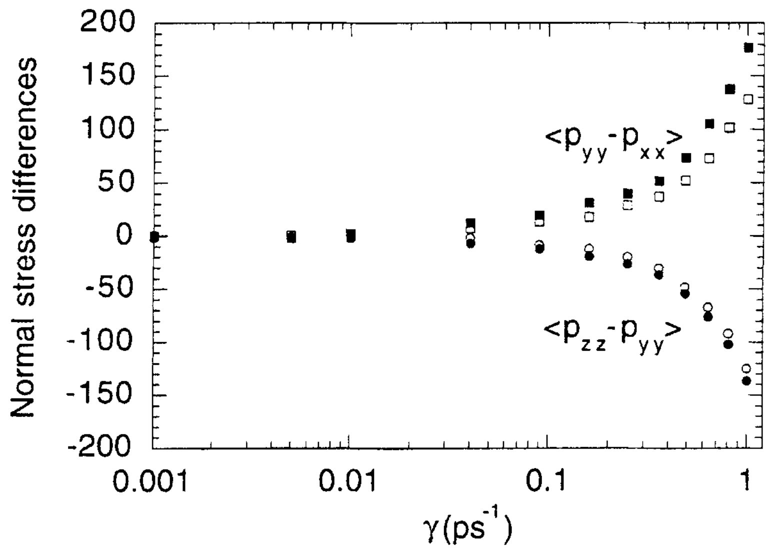

FIGURE 3 The strain rate dependent normal stress difference (MPa) at 296 K and 0.782 g/cc. Black ones: 6-propyl duodecane and open ones: 5-dibutyl nonane.

[36] has devised a convenient representation of normal stress effects by defining the material functions Ψ_1 and Ψ_2, which are related to normal stress differences by $\Psi_1\gamma^2 = P_{yy} - P_{xx}$ and $\Psi_2\gamma^2 = P_{zz} - P_{yy}$. The signs of the material functions for 6-propyl duodecane and 5-dibutyl nonane are consistent with the experimental shear flow, that is $\Psi_1 > 0$ and $\Psi_2 < 0$. This ratio Ψ_2/Ψ_1 varies with strain rate. It is between -0.62 and -0.78 for 6-propyl duodecane and between -0.65 and -0.98 for 5-dibutyl nonane at strain rate of $> 0.09\,\mathrm{ps}^{-1}$. Experiment gives values of ≥ -0.4 [36]. At high strain rate ($0.16 \sim 1.0\,\mathrm{ps}^{-1}$), when the normal stress difference of both 6-propyl duodecane and 5-dibutyl nonane is plotted *vs* $\gamma^{3/2}$ (not shown), it shows a 3/2 power law, but at low strain rate ($< 0.09\,\mathrm{ps}^{-1}$), the normal stress difference *vs* $\gamma^{3/2}$ varies as a curve.

In Figure 4, we plot the strain rate dependent square of radius of gyration for 6-propyl duodecane and 5-dibutyl nonane at 296 K and 0.782 g/cc. The equilibrium value of R_g^2 is 16.26 A^2 for 6-propyl duodecane and 10.93 A^2 for 5-dibutyl nonane. As can be seen from the figures, the overall trend of the radius of gyration is a decrease with strain rate. For 6-propyl duodecane, the square of radius of gyration is not changed at the smallest strain rate, but it is decreased, not changed, and decreased again with strain rate. The variation with strain rate is not regular, which reflects that the molecules are under various conformation with different percentage of C—C—C—C *trans*, shown in Figure 5, and with shear induced stretching and bending. On

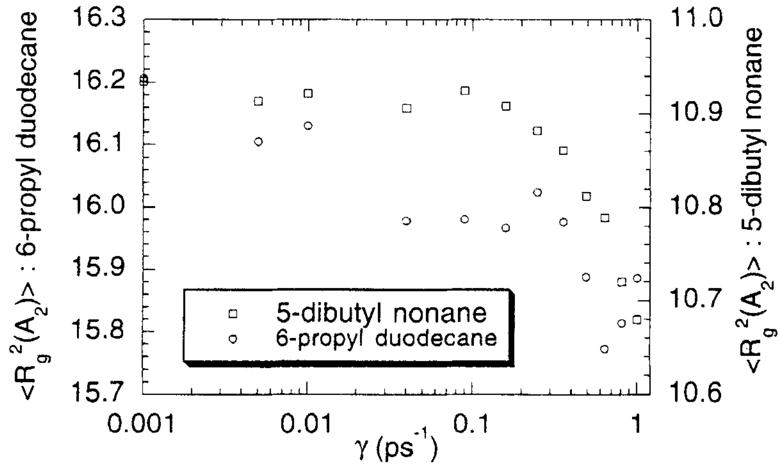

FIGURE 4 The strain rate dependent square of radius of gyration (A^2) for 6-propyl duodecane and 5-dibutyl nonane at 296 K and 0.782 g/cc.

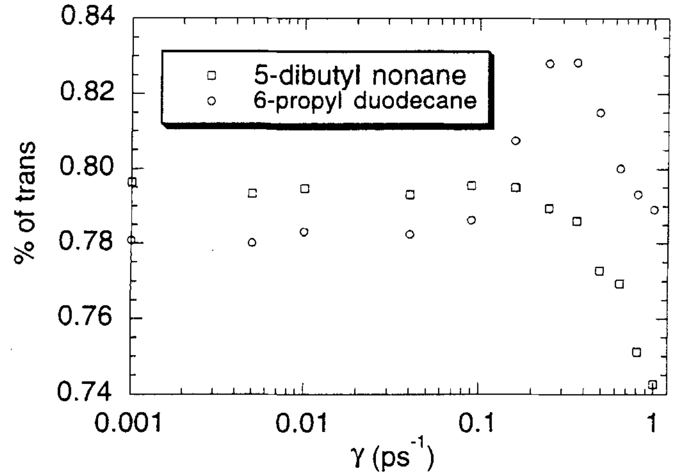

FIGURE 5 The strain rate dependent percentage of C—C—C—C *trans* for 6-propyl duodecane and 5-dibutyl nonane at 296 K and 0.782 g/cc.

the other hand, for 5-dibutyl nonane, the variation of R_g^2 with strain rate is very small at low strain rate (0.001 ~ 0.16 ps^{-1}), not much different from the equilibrium value. This reflects that the chain is very stiff for such branched-chain alkane at low strain rate. For strain rate larger than 0.16 ps^{-1}, however, the square of radius of gyration is nearly linearly decreased with strain rate, which suggests that the average percentage of C—C—C—C *trans* is decreased with strain rage.

Figure 5 shows the strain rate dependent percentage of C—C—C—C *trans* for 6-propyl duodecane and 5-dibutyl nonane at 296 K and 0.782 g/cc. Because of 3 doubly and 4 triply imposed torsional rotational potentials on the bonds of the branched-chain alkanes, the central 6 dihedral states of 6-propyl duodecane and 12 dihedral states of 5-dibutyl nonane are almost fixed among 16 and 20 dihedral states and so only 10 and 8 dihedral states, respectively, are averaged. For 5-dibutyl nonane, the average percentage of C—C—C—C *trans* as a function of strain rate is in excellent correlation with the square of radius of gyration as seen in Figures 4 and 5. For 6-propyl duodecane, the situation is not so simple; two factors are involved since 6-propyl duodecane has a main backbone chain and a branched chain. In general, chains of straight-chain alkanes are stretched with strain rate and the square of radius of gyration is increased with strain rate, while average percentage of C—C—C—C *trans* of branched-chain alkanes is decreased with strain rate and the square of radius of gyration is decreased with strain rate. At low strain rate, the former and the latter are competitive, and at high strain rate the latter dominates for 6-propyl duodecane.

IV. CONCLUSION

We have reported the rheological properties of 6-propyl duodecane and 5-dibutyl nonane at 296 K and 0.782 g/cc. It is found that the Newtonian viscosity can be extrapolated from the plateau value of the strain rate dependent viscosity at low strain rate as the same in straight-chain alkanes [9]. More-branched alkanes have a larger viscosity than less-branched C_{17} alkanes. At high strain rate, two shear thinning regions are observed with different slopes for 6-propyl duodecane and 5-dibutyl nonane, which is characterized as a rheological behavior of branched-chain alkanes, different from that of straight-chain alkanes [9].

Acknowledgement

This research was supported by the Korea Research Foundation through Non-Directed Research Fund, 1994. The author thanks the Korea Institute of Sciences and Technology for the access to the Cray-C90 super computer and the Tongmyung University of Information Technology for the access to its IBM SP/2 computers.

References

[1] Cummings, P. T. and Evans, D. J. (1992). "Nonequilibrium molecular dynamics approaches to transport properties and non-Newtonian fluid rheology", *Ind. Eng. Chem. Res.*, **31**, 1237.

[2] Edberg, R., Morriss, G. P. and Evans, D. J. (1987). "Rheology of *n*-alkanes by nonequilibrium molecular dynamics", *J. Chem. Phys.*, **86**, 4555.

[3] Morriss, G. P., Daivis, P. J. and Evans, D. J. (1991). "The rheology of *n*-alkanes: Decane and eicosane", *J. Chem. Phys.*, **94**, 7420.

[4] Daivis, P. J., Evans, D. J. and Morriss, G. P. (1992). "Computer simulation study of the comparative rheology of branched and linear alkanes", *J. Chem. Phys.*, **97**, 616.

[5] Daivis, P. J. and Evans, D. J. (1994). "Comparison of constant pressure and constant volume nonequilibrium simulations of sheared model decane", *J. Chem. Phys.*, **100**, 541.

[6] Rowley, R. L. and Ely, J. F. (1991). " Non-equilibrium molecular dynamics simulations of structured molecules: Part I. Isomeric effects on the viscosity of butnaes", *Mol. Phys.*, **72**, 831.

[7] Andersen, H. C., Chandler, D. and Weeks, J. D. (1972). "Roles of repulsive and attractive forces in liquids: The optimized random phase approximation", *J. Chem. Phys.*, **56**, 3812.

[8] Andersen, H. C., Chandler, D. and Weeks, J. D. (1976). "Roles of the repulsive and attractive forces in liquids. The equilibrium theory of classical fluids", *Adv. Chem. Phys.*, **34**, 105.

[9] Cui, S. T., Gupta, S. A., Cummings, P. T. and Cochran, H. D. (1996). "Molecular dynamic simulations of the rheology of normal decane hexadecane, and tetracosane", *J. Chem. Phys.*, **105**, 1214.

[10] Lee, S. H. and Cummings, P. T. (1996). "The rheology of *n*-butane and *i*-butane by non-equilibrium molecular dynamics simulations", *Mol. Sim.*, **16**, 229.

[11] Lee, S. H. and Cummings, P. T. (1998). "The rheology of *n*-decane and 4-propyl heptane by non-equilibrium molecular dynamics simulations", *Mol. Sim.*, **21**, 27.

[12] Lee, S. H., Lee, H., Pak, H. and Rasaiah, J. C. (1996). "Molecular dynamics simulation of liquid alkanes. I. Thermodynamics and structures of normal alkanes: *n*-butane to *n*-heptadecane", *Bull. Kor. Chem. Soc.*, **17**, 735.

[13] Lee, S. H., Lee, H. and Pak, H. (1997). "Molecular dynamics simulation of liquid alkanes. II. Dynamics properties of normal alkanes: *n*-butane to *n*-heptadecane", *Bull. Kor. Chem. Soc.*, **18**, 478.

[14] Lee, S. H., Lee, H. and Pak, H. (1997). "Molecular dynamics simulation of liquid alkanes. III. Thermodynamic, structural, and dynamic properties of branched-chain alkanes", *Bull. Kor. Chem. Soc.*, **18**, 501.

[15] Chynoweth, S., Klomp, U. C. and Michopoulos, Y. (1991). "Comment on: Rheology of *n*-alkanes by nonequilibrium molecular dynamics", *J. Chem. Phys.*, **95**, 3024.

[16] Mundy, C. J., Siepman, J. I. and Klein, M. L. (1995). "Calculation of the shear viscosity of decane using a reversible multiple time-step algorithm", *J. Chem. Phys.*, **102**, 3376.

[17] Cui, S. T., Cummings, P. T. and Cochran, H. D. (1996). "Multiple time step non-equilibrium molecular dynamics simulation of the rheological properties of liquid *n*-decane", *J. Chem. Phys.*, **104**, 255.

[18] Chynoweth, S., Klomp, U. C. and Scales, L. E. (1991). "Simulation of organic liquids using pseudo-pairwise interatomic forces on a toroidal transputer array", *Comput. Phys. Commun.*, **62**, 297.

[19] Ryckaert, J. P. and Bellemans, A. (1978). "Molecular dynamics of liquid alkanes", *Discuss. Faraday Soc.*, **66**, 95.

[20] Edberg, R., Evans, D. J. and Morriss, G. P. (1986). "Constrained molecular dynamics: Simulations of liquid alkanes with a new algorithm", *J. Chem. Phys.*, **84**, 6933.

[21] White, D. N. J. and Boville, M. J. (1977). "Molecular mechanics calculations on alkanes and non-conjugated alkanes", *J. Chem. Soc., Perkin Trans.*, **2**, 1610.

[22] Evans, D. J. and Morriss, G. P. (1984). "Nonlinear response theory for steady planar Couette flow", *Phys. Rev. A*, **30**, 1528; ibid, "Non-Newtonian molecular dynamics", *Comput. Phys. Repts.*, **1**, 297.

[23] Lees, A. W. and Edwards, S. F. (1972). "The computer study of transport processes under extreme conditions", *J. Phys. C: Solid State*, **5**, 1921.

[24] Muller-Plathe, F., Rogers, S. C. and van Gunsteren, W. F. (1993). "Gas sorption and transport in polyisobutylene: Equilibrium and nonequilibrium molecular dynamics simulations", *J. Chem. Phys.*, **98**, 9895.

[25] Evans, D. J., Hoover, W. G., Failor, B. H., Moran, B. and Ladd, A. J. C. (1983). "Nonequilibrium molecular dynamics *via* Gauss's principle of least constraint", *Phys. Rev. A*, **28**, 1016.

[26] Simmons, A. D. and Cummings, P. T. (1986). "Non-equilibrium molecular dynamics simulation of dense fluid methane", *Chem. Phys. Lett.*, **129**, 92.

[27] Gear, C. W. (1971). *Numerical Initial Value Problems in Ordinary Differential Equation* (Prentice-Hall, Englewood Cliffs, NJ).

[28] Berker, A., Chynoweth, S., Klomp, U. C. and Michopoulos, Y. (1992). "Non-equilibrium molecular dynamics (NEMD) simulations and the rheology properties of liquid *n*-hexadecane", *J. Chem. Soc. Faraday Trans.*, **88**, 1719.

[29] Yamada, T. and Kawasaki, K. (1975). "Application of mode-coupling theory to nonlinear stress tensor in fluids", *Prog. Theor. Phys.*, **53**, 111.

[30] Kawasaki, K. and Gunton, J. D. (1973). "Theory of nonlinear transport processes: Nonlinear shear viscosity and normal stress effects", *Phys. Rev. A*, **8**, 2048.

[31] Ernst, M. H., Cichocki, B., Dorfman, J. R., Sharma, J. and van Beijeren, H. J. (1978). "Kinetic theory of nonlinear viscous flow in two and three dimensions", *J. Stat. Phys.*, **18**, 237.

[32] Lee, S. H. and Cummings, P. T. (1993). "Shear viscosity of model mixtures by nonequilibrium molecular dynamics. I. Argon-krypton mixtures", *J. Chem. Phys.*, **99**, 3919.

[33] Lee, S. H. and Cummings, P. T. (1994). "Effect of three-body forces on the shear viscosity of liquid argon", *J. Chem. Phys.*, **101**, 6206.

[34] Lee, S. H. and Cummings, P. T. (1996). "Shear viscosity of model mixtures by nonequilibrium molecular dynamics. II. Effect of dipolar interactions", *J. Chem. Phys.*, **105**, 2044.

[35] Clarke, J. H. and Brown, D. (1987). "The rheological properties of liquids composed of flexible chain molecules: a molecular dynamics simulation study", *J. Chem. Phys.*, **86**, 1542.

[36] Bird, R. B., Hassager, O., Amstrong, R. C. and Curtiss, C. F. (1977). *Dynamics of Polymeric Liquids Vol. 1: Fluid Mechanics* 2nd ed. (Wiley, New York); Bird, R. B., Hassager, O., Amstrong, R. C. and Curtiss, C. F., *Dynamics of Polymeric Liquids Vol. 2: Kinetic Theory*, 2nd ed. (Wiley, New York, 1977).